Effect of ^{13}C isotope doping on the optical phonon modes in graphene: Localization and Raman spectroscopy

J. F. Rodriguez-Nieva,[1,2] R. Saito,[3] S. D. Costa,[4] and M. S. Dresselhaus[1,5]

[1]*Department of Physics, Massachusetts Institute of Technology, Cambridge, Massachusetts 02139, USA*

[2]*Department of Materials Science and Engineering, Massachusetts Institute of Technology, Cambridge, Massachusetts 02139, USA*

[3]*Department of Physics, Tohoku University, Sendai, 980-8578 Japan*

[4]*Departamento de Física, Universidade Federal de Minas Gerais, 30123-970 Belo Horizonte, Brazil*

[5]*Department of Electrical Engineering and Computer Science, Massachusetts Institute of Technology, Cambridge, Massachusetts 02139-4307, USA*

(Received 12 April 2012; published 5 June 2012)

The effect of ^{13}C isotope impurities on the phonon properties of graphene is discussed theoretically. We calculated the values of the phonon lifetimes due to isotope impurity scattering for all values of densities, isotopic masses, and for all wave vectors using second-order perturbation theory. We found that for natural concentrations of ^{13}C, the contribution of isotopic scattering to the phonon lifetime of the optical modes is negligible when compared to the electron-phonon interaction. Nevertheless, for atomic concentrations of ^{13}C as high as $\rho = 0.5$ both contributions become comparable. Our results are compared with recent experimental results and we find good agreement both in the ^{13}C atomic density dependence of the lifetime as well as in the calculated spectral width of the G-band. Due to phonon scattering by ^{13}C isotopes, some graphene phonon wave functions become localized in real space. Numerical calculations show that phonon localized states exist in the high-energy optical phonon modes and in regions of flat phonon dispersion. In particular, for the case of in-plane optical phonon modes, a typical localization length is on the order of 3 nm for ^{13}C atomic concentrations of $\rho \approx 0.5$. Optical excitation of phonon modes may provide a way to experimentally observe localization effects for phonons in graphene.

DOI: 10.1103/PhysRevB.85.245406 PACS number(s): 63.20.kp, 63.22.Rc, 78.30.−j

I. INTRODUCTION

The ^{13}C isotope exists in natural carbon in a 1.1% abundance and the remaining 98.9% are ^{12}C. Because of the low concentration of ^{13}C, we can usually neglect this isotope effect for discussing the physical properties of graphene-related materials. However, if we consider, for example, the intrinsic spectral linewidth in Raman spectroscopy, the isotope effect might be essential as one of the important intrinsic scattering mechanisms. When we intentionally increase the ^{13}C isotope concentration in an sp^2 material, the graphene-related material made of varying concentrations of ^{13}C has provided interesting information for better understanding of phonon related properties[1] as well as growth mechanisms.[2,3] The advantage of the isotope enrichment technique is that only phonon frequencies or thermal properties can be modified without changing the electrical or chemical properties, so that we can distinguish the electron-phonon interaction from electronic or electron-electron interactions in making assignments for unassigned optical spectral features.[1] In the case of crystal growth, if we substitute a ^{12}C atom in a gas source molecule by a ^{13}C atom, we can get information on how the carbon atoms from the gas molecule are used for the crystal growth of carbon nanotubes[2] and graphene.[3]

Miyauchi *et al.*[1] made a 100% ^{13}C single wall nanotube (SWNT) sample by chemical vapor deposition using ^{13}C ethanol. Comparing the Raman spectra of ^{13}C SWNTs and ^{12}C SWNTs, they assigned the phonon-assisted peaks in the photoluminescence spectra. Kalbac *et al.*[4] observed the Raman spectra of a special bilayer graphene sample on a substrate in which the top (bottom) layer of the bilayer graphene consisted of pure ^{12}C (^{13}C) so that they could separately investigate the single-layer components of bilayer graphene. Costa *et al.*[5] observed a frequency shift and broadening of the Raman G band in single-wall carbon nanotubes as a function of ^{13}C concentration, and they suggested that these effects were caused by phonon localization due to the elastic scattering of phonons by the ^{13}C atoms.[5] In addition, they studied the laser energy dependence of the G′ and D bands for pure ^{12}C and pure ^{13}C samples. They found for each band that the slope of the curve, which is sensitive to the electronic structure, does not change with the isotope mass. This result serves as strong experimental evidence that isotope enrichment does not modify the electronic structure.

Many theoretical works are focused on thermal transport properties of isotope-enriched samples. Savić *et al.*[6] studied the phonon transport of isotope disordered SWNTs and boron nitride nanotubes in the presence of isotope disorder by an *ab initio* calculation. They calculated the reduction in thermal conductivity due to the impurities, and they concluded that the reduction is mostly due to diffusive scattering of phonons by the isotopes. More recently, Yamamoto *et al.*[7] extended the previously mentioned calculations to study phonon transmission fluctuations in carbon nanotubes, finding a universal behavior with respect to phonon transmission, tube chirality, and concentrations and masses of isotopes. In these two works,[6,7] the three transport regimes (ballistic, diffusive, and localized) are observed, and localization lengths are calculated via atomistic Green's function formalisms, while localization effects of the phonon wave function are not discussed. As pointed out by Savić *et al.*, localization effects are difficult to observe in thermal transport measurements because the thermal conductance is mostly dominated by the ballistic and diffusive contributions. The localization regime appears in the high-energy optical modes, and thus special

experimental techniques capable of probing these high-energy modes are required to observe any localization effects.

We are here interested in optical phonon scattering and the localization effect in graphene, which are the main topics of the present paper. Phonon localization is another example of Anderson's localization theory,[8,9] which is applicable to several wave phenomena like light[10] or water waves,[11] but has in the past been mostly associated with electronic transport in disordered crystals. When the phonon wave function is localized, the phonon mean free path λ_{ph} becomes finite and proportional to the square of the localization length λ.

When we discuss the electron-phonon interaction of graphene,[12,13] we generally treat the phonon wave function as delocalized in the crystal. However, in a real graphene sample, we know that 1.1% of the atoms are ^{13}C and thus phonons have a finite lifetime τ and a finite localization length λ due to the phonon scattering by ^{13}C, which is one of the main contributions to the natural linewidth γ of the Raman spectra. Further, we need theoretical understanding on how the localization length λ of the phonon is changed as a function of ^{13}C concentration so that we can explain the experimental observations of Costa *et al.*[5]

In this work, we calculate the phonon wave function in a large unit cell, large enough so that the localization length λ is smaller than the size of this unit cell. When we add an impurity to a perfect crystal lattice, the translational symmetry is broken, and the wave vectors associated with the unit cell are no longer good quantum numbers. This means that phonons are scattered into other states, and some of the wave functions are localized in real space by mixing many q states, where q is the phonon wave vector.

It should be mentioned that the anharmonicity of the vibration also produces phonon scattering. However, in this paper, we do not discuss this effect for simplicity. Since the anharmonicity effect should be significant for large phonon amplitudes, this phenomenon is important only for high temperatures and can, in principle, be tuned in experiments.

Our objective in the present work is twofold. On the one hand, we calculate the optical phonon lifetimes due to impurity scattering in order to have a value to compare with competing processes. The advantage of performing this estimation is that, assuming all scattering processes to be independent (Matthiessen's rule), our calculation of λ provides a way to directly compare the lifetimes of the different interactions that are important for phonon properties, such as the electron-phonon interaction. Additionally, we calculate the localization length as a function of impurity density to study localization effects caused by isotope impurities. We focus particularly on the LO and iTO modes because of their importance in the Raman G band, the dominant feature in the first order spectra.

The outline of this paper is as follows. In Sec. II, we briefly introduce the theoretical background necessary for the calculation of phonon lifetimes and localization lengths. In Sec. III, we show the calculated results for phonon lifetimes as a function of ^{13}C isotope concentration and for the different wave vectors in the Brillouin zone (BZ). We compare our calculated results with the experimental values obtained by Costa *et al.*[5] and we also calculate the phonon localization length λ as a function of phonon frequency ω. In Sec. IV, a summary of the present work is given.

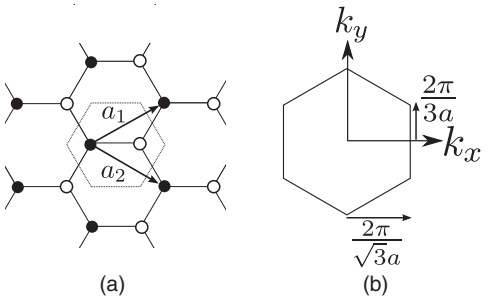

FIG. 1. (a) Unit cell of graphene and the translation vectors a_1 and a_2. (b) The BZ of graphene. Here, a is the lattice constant of graphene (0.246 nm).

II. THEORETICAL BACKGROUND

We solve the phonon lifetime and localization problem within the harmonic approximation in which up to fourth-nearest-neighbor interactions are considered and using the force constants of Jishi *et al.*[14] The unit cell and the BZ of graphene are shown in Fig. 1. The effect of adding a ^{13}C isotope impurity to the lattice will not modify the force constant parameters, as the extra neutron in each nucleus will not modify the chemistry of the bonding. However, the isotope impurity will affect the dynamics due to the increased mass of the ion which is incorporated into the perturbed Hamiltonian. In Sec. II A, we briefly describe the solution to the unperturbed problem, in which we obtain expressions that will be useful for calculating phonon lifetimes, and in Sec. II B, we describe the model we used for estimation of phonon lifetimes.

A. Unperturbed Hamiltonian

The unperturbed Hamiltonian of phonons, within the harmonic approximation, is given by

$$H = \sum_{i,\nu} \frac{\mathbf{p}_i^\nu \cdot \mathbf{p}_i^\nu}{2m_\nu} + \sum_{i,j,\nu,\nu'} \frac{\mathbf{u}_i^\nu \Phi_{ij}^{\nu\nu'} \mathbf{u}_j^{\nu'}}{2}, \tag{1}$$

where the subscripts i, j label the unit cell in the supercell and ν labels the atom within the unit cell (i.e., $i = 1,2,\ldots,N$, and $\nu = 1,2$, which corresponds to the graphene sublattice A or B, respectively) and $\mathbf{u}_i^\nu$ and $\mathbf{p}_i^\nu$ are the amplitude and momentum of vibrations at the (i,ν)th atom, respectively. The term $\Phi_{ij}^{\nu\nu'}$ is the interaction potential between the atoms at (i,ν) and (j,ν'), and m_ν is the mass of the atom at site ν within the unit cell. $\mathbf{u}_i^\nu$ and $\mathbf{p}_i^\nu$ satisfy the commutation relation $[u_{il}^\nu, p_{jl'}^{\nu'}] = i\hbar\delta_{ij}\delta_{\nu\nu'}\delta_{ll'}$, where $l,l' = x,y,z$. $\mathbf{u}_i^\nu$ and $\mathbf{p}_i^\nu$ can be expressed by a Fourier transformation for wave vectors q within the BZ:

$$\mathbf{u}_i^\nu = \sum_q \frac{e^{iq\cdot r_i^\nu}}{\sqrt{N}} \mathbf{u}_q^\nu, \tag{2}$$

and

$$\mathbf{p}_i^\nu = \sum_q \frac{e^{-iq\cdot r_i^\nu}}{\sqrt{N}} \mathbf{p}_q^\nu, \tag{3}$$

where r_i^ν is the equilibrium position of atom (i,ν). Then Eq. (1) can be expressed in terms of q:

$$H = \sum_{q,\nu} \frac{\mathbf{p}_q^\nu \cdot \mathbf{p}_q^{\nu\dagger}}{2m_\nu} + \sum_{q,\nu,\nu'} \frac{\mathbf{u}_q^{\nu\dagger} \Phi_q^{\nu\nu'} \mathbf{u}_q^{\nu'}}{2}, \tag{4}$$

where $\Phi_q^{\nu\nu'} = \sum_j \Phi_{ij}^{\nu\nu'} e^{iq\cdot(r_j^{\nu'} - r_i^{\nu'})}$. We diagonalize the Fourier transform of the interaction potential Φ_q according to

$$\sum_{\nu'} \frac{\Phi_q^{\nu\nu'}}{\sqrt{m_\nu m_{\nu'}}} \mathbf{e}_{qn}^{\nu'} = \omega_{qn}^2 \mathbf{e}_{qn}^{\nu}, \tag{5}$$

where ω_{qn} ($\mathbf{e}_{qn}$) is the eigenvalue (eigenvector) of the nth normal phonon mode for wave vector q. The eigenvectors satisfy the normalization condition $\sum_\nu \mathbf{e}_{qn}^{\nu*} \cdot \mathbf{e}_{qn'}^{\nu} = \delta_{nn'}$. Further, we define the displacement of the nth normal mode with wave vector q by

$$X_{qn} = \sum_\nu \sqrt{m_\nu} \mathbf{e}_{qn}^{\nu*} \cdot \mathbf{u}_q^\nu, \tag{6}$$

and, similarly, for the momentum,

$$P_{qn} = \sum_\nu \frac{1}{\sqrt{m_\nu}} \mathbf{e}_{qn}^{\nu} \cdot \mathbf{p}_q^\nu. \tag{7}$$

The Hamiltonian of Eq. (4) is thus simplified to

$$H = \sum_{q,n} \frac{P_{qn} P_{qn}^\dagger}{2} + \frac{\omega_{qn}^2 X_{qn}^\dagger X_{qn}}{2}, \tag{8}$$

where $[X_{qn}, P_{q'n'}] = i\hbar\delta_{qq'}\delta_{nn'}$. Finally, we define the annihilation and creation operators, respectively, as

$$a_{qn} = \sqrt{\frac{\omega_{qn}}{2\hbar}} (X_{qn} + i P_{qn}^\dagger/\omega_{qn}), \tag{9}$$

and

$$a_{qn}^\dagger = \sqrt{\frac{\omega_{qn}}{2\hbar}} (X_{qn}^\dagger - i P_{qn}/\omega_{qn}), \tag{10}$$

which satisfy $[a_{qn}, a_{q'n'}^\dagger] = \delta_{qq'}\delta_{nn'}$. The Hamiltonian now becomes

$$H = \sum_{qn} \hbar\omega_{qn} \left(a_{qn}^\dagger a_{qn} + \frac{1}{2} \right). \tag{11}$$

B. Estimation of the phonon lifetime

There are two ways to calculate the phonon lifetime for each phonon mode. In the first approach, we can use the eigenstates and eigenvalues found for a large graphene supercell and use these values to determine the T matrix.[15] In the second approach, we can treat the change in the mass matrix as a perturbation and find the phonon lifetime using perturbation theory. We use the second approach to gain better physical insight and to obtain explicit analytic expressions.

If we add ^{13}C isotope impurities into the lattice, we can consider the Hamiltonian in Eq. (1) in which we set the mass m_ν equal to the average mass $\bar{m} = \sum_{i,\nu} m_{i,\nu}/2N$. Then, the perturbation to the Hamiltonian ΔH is due to the kinetic term (expressed in terms of velocities) and given by

$$\Delta H = \sum_{j\nu'} \frac{f_j^{\nu'}}{2} \bar{m} \dot{\mathbf{u}}_j^{\nu'} \cdot \dot{\mathbf{u}}_j^{\nu'}, \tag{12}$$

where $f_j^{\nu'} = (m_j^{\nu'} - \bar{m})/\bar{m}$. We can express Eq. (2) in terms of creation and annihilation operators a_{qn} and $a_{qn}^\dagger$ using Eqs. (9) and (10),

$$\mathbf{u}_j^{\nu'} = \sum_{qn} \sqrt{\frac{\hbar}{2N\bar{m}\omega_{qn}}} e^{iq\cdot r_j^{\nu'}} (a_{qn} + a_{-qn}^\dagger) \mathbf{e}_{qn}^{\nu'}, \tag{13}$$

and then replace Eq. (13) in Eq. (12) to obtain

$$\Delta H = \sum_{qq'nn'} h_{qq'}^{nn'} (a_{qn} a_{-q'n'}^\dagger + a_{-qn}^\dagger a_{q'n'}), \tag{14}$$

where we dropped the terms involving the product of two creation (annihilation) operators as they do not conserve energy. These two terms that were dropped are going to be relevant beyond second-order perturbation theory. The amplitude for scattering a phonon from q to q', denoted by $h_{qq'}^{nn'}$, is given by

$$h_{qq'}^{nn'} = \frac{\hbar R(q,q')}{4N} \sqrt{\omega_{qn}\omega_{q'n'}} \sum_{\nu'} \mathbf{e}_{qn}^{\nu'} \cdot \mathbf{e}_{q'n'}^{\nu'}, \tag{15}$$

where $R(q,q') = \sum_j f_j^{\nu'} e^{i(q+q')\cdot r_j^{\nu'}}$ is the phase factor. We can use the Fermi golden rule to determine the transition rates $P_{i\to f}$ for phonon scattering from the initial (i) to final state (f),

$$P_{i\to f} = \frac{2\pi}{\hbar} |\langle f|\Delta H|i\rangle|^2 \delta(E_f - E_i), \tag{16}$$

within second-order perturbation theory. The transition probability for scattering from state (q,n) to (q',n') is given by

$$P_{qq'}^{nn'} = \frac{2\pi}{\hbar} N_{qn}(N_{q'n'} + 1) \left| h_{qq'}^{nn'} \right|^2 \delta(\hbar\omega_{qn} - \hbar\omega_{q'n'}), \tag{17}$$

where N_{qn} ($N_{q'n'}$) is the number of phonons in state (q,n) $[(q',n')]$, and the lifetime of the phonon mode (q,n) is then given by

$$\tau_{qn}^{-1} = \frac{\pi}{2N^2} \sum_{q'n'} |R(q,q')|^2 \omega_{qn}\omega_{q'n'} (\mathbf{e}_{qn}^* \cdot \mathbf{e}_{q'n'})^2 \delta(\omega_{qn} - \omega_{q'n'}). \tag{18}$$

Because we assume that the impurities are randomly distributed, we can use the random phase approximation to evaluate $|R(q,q')|^2$. If we take an ensemble average of $|R(q,q')|^2$ over different realizations of the isotopically doped samples

$$\langle |R(q,q')|^2 \rangle = \left\langle \sum_{j,l} f_j^{\nu'} f_l^{\nu'} e^{i(q+q')\cdot(r_j^{\nu'} - r_l^{\nu'})} \right\rangle, \tag{19}$$

we obtain

$$\langle |R(q,q)|^2 \rangle = \sum_j f_j^{\nu'} f_j^{\nu'} = \frac{N\Delta m^2 \rho(1-\rho)}{(m_0 + \rho\Delta m)^2}, \tag{20}$$

where ρ is the number density of ^{13}C ($0 \leqslant \rho \leqslant 1$), m_0 is the mass of ^{13}C, and Δm is the mass difference between ^{12}C and

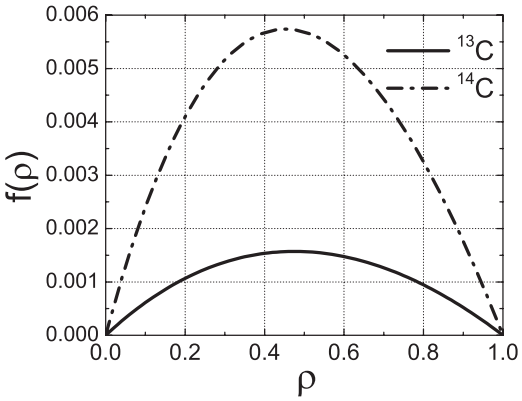

FIG. 2. Density dependence of the lifetime given by the function $f(\rho)$ as defined in Eq. (22).

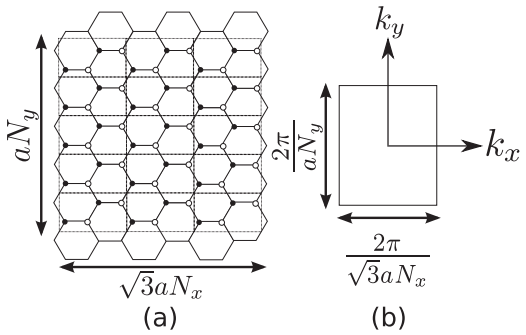

FIG. 3. (a) An example of a supercell, with $N = 30$ unit cells and 60 carbon atoms. Here, N_x and N_y label the number of unit cells in the x and y directions, respectively. (b) The BZ of this supercell.

^{13}C isotopes. We discussed previously that our unperturbed Hamiltonian of Eq. (1) is the one corresponding to the average mass $\bar{m}$ so that the frequency spectrum is equivalent to the one corresponding to pure ^{12}C but scaled as $\propto (\bar{m})^{-1/2}$ in the case of general ρ. Thus, if we rescale frequencies as $\omega = \omega^0\sqrt{\bar{m}/m_0}$, where m_0 is the mass of ^{12}C, we can factorize the density ρ and isotope mass dependence $(m_0 + \Delta m)$ from the summation in Eq. (18), yielding a phonon lifetime

$$\tau_{qn}^{-1} = \frac{\pi f(\rho)}{2N} \sum_{q'n'} \omega_{qn}^0 \omega_{q'n'}^0 (\mathbf{e}_{qn}^* \cdot \mathbf{e}_{q'n'})^2 \delta\left(\omega_{qn}^0 - \omega_{q'n'}^0\right), \quad (21)$$

where the frequencies ω_{qn}^0 correspond to the nth phonon mode frequency at q of ^{12}C. The function $f(\rho)$ contains all the information about isotope mass and density:

$$f(\rho) = \frac{\Delta m^2 \rho(1-\rho)}{(m_0 + \rho\Delta m)^2} \sqrt{\frac{m_0}{m_0 + \rho\Delta m}}. \quad (22)$$

The function $f(\rho)$ is plotted versus isotope density ρ in Fig. 2 for the cases of ^{13}C and ^{14}C. Here, we see that the effect of using ^{14}C instead of ^{13}C produces a reduction of the lifetime by a factor of approximately 4. ^{14}C is an unstable isotope, while ^{13}C is stable and is found in naturally occurring materials. Thus we focus on ^{13}C for the rest of the paper. Nevertheless, we keep in mind that using ^{14}C just changes the prefactor of Eq. (21) as plotted in Fig. 2. In addition, we can transform Eq. (18) into an integral over the BZ, yielding

$$\tau_{qn}^{-1} = \frac{f(\rho) S}{8\pi} \sum_{n'} \int d^2q' \omega_{qn}^0 \omega_{q'n'}^0 (\mathbf{e}_{qn}^* \cdot \mathbf{e}_{q'n'})^2 \delta\left(\omega_{qn}^0 - \omega_{q'n'}^0\right), \quad (23)$$

where S is the area of the unit cell. Here we emphasize again that the term inside the summation of Eq. (23) has no dependence on impurity density or isotope mass, so that the integration of Eq. (23) can be done using pure ^{12}C eigenstates and eigenvalues, independent of the particular isotopically doped sample we are considering. Therefore we can express Eq. (23) as

$$\tau_{qn}^{-1}(\rho) = f(\rho) I_{qn}, \quad (24)$$

where the function $f(\rho)$ contains the density ρ dependence of the lifetime, while I_{qn} contains the wave vector (and frequency) dependence and gives the correct units of s^{-1}. The value of I_{qn} is increased as we go to modes with higher frequencies and in points of the BZ with high density of states. In the next sections, we will drop the superscripts 0 in Eq. (23) but taking into account that we are referring to the eigenstates and eigenvalues of a pure sample containing only ^{12}C atoms. Equation (24) is the result of using second-order perturbation theory and the random phase approximation. Inclusion of higher-order terms in the perturbation expansion will result in a more complicated expression of the phonon lifetime in Eq. (24) in which the ρ density dependence can no longer be factorized.

C. Localized states

To estimate the localization length λ of the localized states, we numerically solve the Hamiltonian of a supercell containing N unit cells of graphene. Even though this approach may become time consuming for unit cells large enough to do quantitative calculations, the advantage of numerically calculating the eigenstates and eigenvalues (as opposed to using perturbation theory) is that we can obtain additional information about the eigenstates that would be difficult to calculate otherwise. An example of the type of supercell consisting of $2N$ atoms that we used in our calculations is shown in Fig. 3. Here, we introduced periodic boundary conditions for the supercell. Because of the breaking of the translational symmetry by the introduction of ^{13}C impurity atoms, we change the labels from $\mathbf{u}_i^\nu$, with $i = 1,2,\ldots,N$ and $\nu = 1,2$, to $\mathbf{u}^\mu$, with $\mu = 1,2,\ldots,2N$. Therefore the displacements $\mathbf{u}^\mu$ in the supercell have $6N$ components. The diagonalization of this problem is analogous to the case of the unperturbed Hamiltonian, but in this case, we diagonalize the large $6N \times 6N$ (real) matrix $\Phi^{\nu\nu'}$ according to

$$\sum_{\mu'} \frac{\Phi^{\mu\mu'}}{\sqrt{m_\mu m_{\mu'}}} \mathbf{e}_j^{\mu'} = \omega_j^2 \mathbf{e}_j^\mu \ (\mu = 1,\ldots,2N; j = 1,\ldots,6N), \quad (25)$$

in which ω_j ($\mathbf{e}_j^\mu$) is the eigenvalue (eigenvector) of the jth normal mode. The orthonormal condition on the eigenvectors $\mathbf{e}_j^\mu$ is given by

$$\sum_{\mu=1}^{2N} \mathbf{e}_j^\mu \cdot \mathbf{e}_{j'}^\mu = \delta_{jj'}. \quad (26)$$

If we have extended states, on average $|\mathbf{e}_j^\mu| \approx 1/\sqrt{N}$. On the other hand, for a highly localized state, we have $|\mathbf{e}_j^\mu| \approx 1$ for only a few atoms and $|\mathbf{e}_j^\mu| \approx 0$ for the rest. Therefore we can distinguish localized states from nonlocalized states by defining the second moment of the displacement field A_j (also known as the inverse participation number[16]) as

$$A_j = \sum_\nu \left(\mathbf{e}_j^\nu \cdot \mathbf{e}_j^\nu\right)^2. \tag{27}$$

Most of the eigenstates will be extended states in which case $A_j \approx 1/N$, while for localized states A_j is much larger and $A_j \approx 1$.

At the same time, the function A_j is also useful to estimate the localization length λ_j of the eigenstates j, since λ_j and A_j are related by $\lambda_j \propto A_j^{-1/2}$.[9] As we know, for the ^{13}C concentration $\rho = 0$, all states are extended states. We can then estimate the localization length of state j by

$$\frac{\lambda_j}{\lambda_0} = \left(\frac{\bar{A}_0}{A_j}\right)^{1/2}, \tag{28}$$

where λ_0 is the size of the supercell and $\bar{A}_0$ is the average value of A_j for the special case of a pristine graphene sample with only ^{12}C atoms. For our calculations, we used a supercell containing $N = 2700$ unit cells ($\lambda_0 \approx 13$ nm) which, for natural carbon, contains 59 impurity atoms.

III. RESULTS

A. Phonon lifetime

We calculated numerically the phonon lifetime for the elastic scattering process using Eq. (23). Even though we do not here intend to discuss acoustic phonon modes, we note that an analytical expression for the lifetime of the acoustic phonon modes can be obtained by similar means and can be found in the literature in relation to discussions of heat transfer.[17] This will be useful to obtain an idea about the order of magnitude of the optical phonon scattering process, but we also calculate numerically the values of τ_{qn}^{-1} from Eq. (23) for all phonon modes. Due to our special interest in the optical modes, we discuss these modes in more detail. Then we can compare the contribution to phonon scattering coming from the presence of isotopic impurities with competing processes contributing to τ_{qn}^{-1}.

1. Low-energy acoustic phonon modes

For the case of low-energy acoustic phonon modes in graphene, we have linear dispersion relations for the LA and iTA modes near the Γ point and a quadratic relation for the oTA mode. The integration of Eq. (23) over reciprocal space can be done analytically for the three acoustic modes. Because of the dot product term in Eq. (23), we have a decoupling in the expression of the in-plane and out-of-plane phonon modes. For the in-plane modes, we use $\omega_{q'n'} \approx c_{n'} q'$ in Eq. (23), where $c_{n'}$ is the velocity of the phonon mode. We can define further an average value over the BZ for the dot product of the polarization for the in-plane modes $p_{\text{in}} = \langle(\mathbf{e}_{qn}^* \cdot \mathbf{e}_{q'n'})^2\rangle$. The exact values for this polarization term in the case of graphene can be found in the paper by Lindsay *et al.*[18]

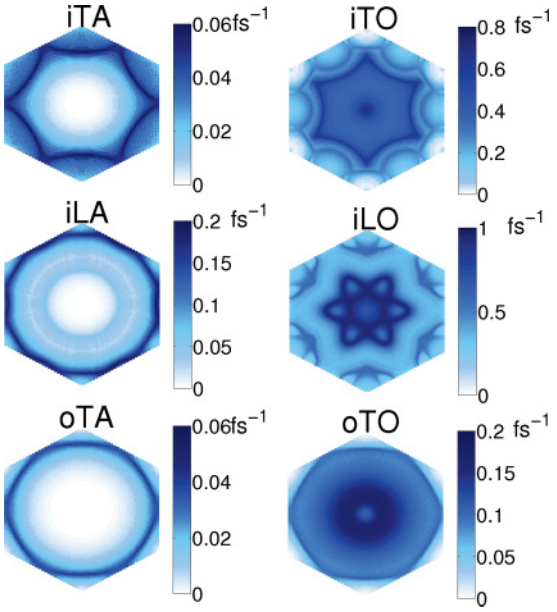

FIG. 4. (Color online) Plot of $I_{qn} = (\tau f)^{-1}$ for the different phonon modes and wave vectors in the two-dimensional BZ as defined in Eq. (24), where $f(\rho)$ is defined in Eq. (22) and plotted in Fig. 2. Intensity scales are plotted beside each mode map. In-plane optical phonon modes (iTO and iLO) are seen to have a significantly lower lifetime than the other modes.

Substituting p_{in} into Eq. (23) and solving the indicated integral, we obtain for the phonon lifetime

$$\tau_{qn}^{-1} = \frac{f(\rho) S p_{\text{in}}}{4}\left(\sum_{n'} c_{n'}^{-2}\right)\omega_{qn}^3 = \frac{f(\rho) S p_{\text{in}}}{2\bar{c}^2}\omega_{qn}^3. \tag{29}$$

Similarly, for the out-of-plane phonon modes using $\omega_{q'} = bq'^2$, and $p_{\text{out}} = \langle(\mathbf{e}_{qn}^* \cdot \mathbf{e}_{q'n'})^2\rangle$ for n =out-of-plane, we obtain for the oTA mode

$$\tau_{qn}^{-1} = \frac{f(\rho) S p_{\text{out}}}{8b}\omega_{qn}^2. \tag{30}$$

The order of magnitude of the phonon lifetime of the optical in-plane modes (LA and iTA) due to isotopic impurities can be estimated by evaluating Eq. (29) at the BZ boundaries and using $S = 0.052$ nm^2, $p_{\text{in}} \approx 0.5$, $\bar{c} \approx 20$ km/s, $\hbar\omega_{qn} \approx 0.15$ eV (ω_{qn} at $q \approx \pi/a$) and evaluating $f(\rho)$ at the desired ^{13}C density. Therefore the order of magnitude of the lifetime of an in-plane optical phonon mode for the natural ^{13}C isotopic density ($\rho = 0.011$) is $\tau \sim 30$ ps, and for a ^{13}C concentration of $\rho = 0.5$, we obtain a much shorter lifetime of $\tau \sim 1$ ps.

2. General phonon lifetime

For the general case of wave vector q and phonon mode n, we do a numerical integration of Eq. (23) over the BZ. The value of $(\tau f)^{-1}$ is plotted as a function of q in the BZ and for all phonon modes in Fig. 4. As discussed in Eq. (24), the value of $(\tau f)^{-1}$ is independent of isotope density or isotope mass and to obtain a numerical value for the phonon lifetime τ, we must first calculate the value of $f(\rho)$ of Eq. (22) from Fig. 2 depending on the particular values of ^{13}C concentrations in the sample. As expected, optical phonon modes are sensitively affected by the isotope impurities, while acoustic modes close

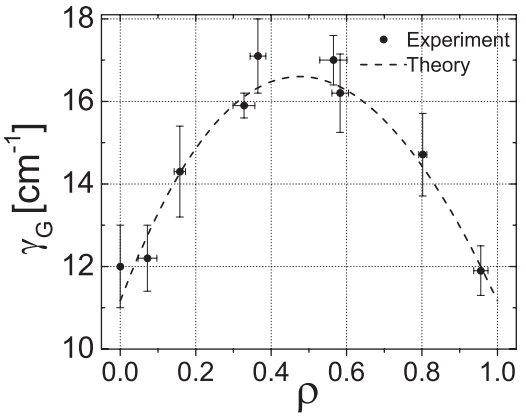

FIG. 5. The points are the experimental values for the spectral width γ_G (FWHM) of the G band obtained by Costa *et al.*[5] and the dashed curve is γ_G obtained by fitting Eq. (31) with the values of $\gamma^{\text{exp}}_{\text{e-ph}} = 11.2 \pm 0.4\ \text{cm}^{-1}$ and $\gamma^{\text{exp}}_{\text{ph-imp}} = 5.2 \pm 0.4\ \text{cm}^{-1}$.

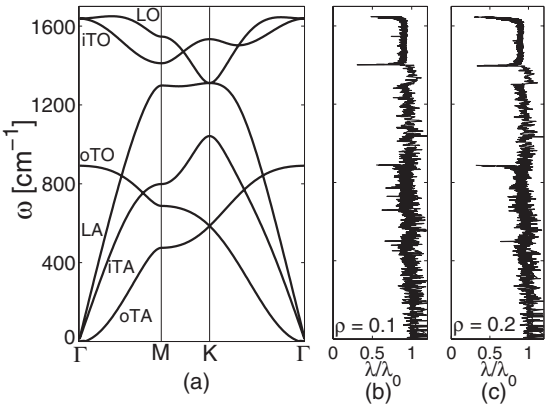

FIG. 6. (a) Phonon dispersion for monolayer graphene.[14] (b) and (c) Normalized localization length λ/λ_0 (λ_0 is the size of super cell) as a function of the phonon frequency for the atomic isotope impurity densities of (b) $\rho = 0.1$ and (c) $\rho = 0.2$ (surface densities of 3.8 and 7.6 nm^{-2}, respectively).

to the Γ point are less affected. For the acoustic modes, and close to the Γ point, we observe the power law behavior obtained in the previous section, i.e., $(\tau f)^{-1} \propto \omega^3 \propto q^3$ for the in-plane modes, and $(\tau f)^{-1} \propto \omega^2 \propto q^4$ for the out-of-plane modes. There is also a large difference in the lifetime scale between in-plane and out-of-plane phonon modes due to the large difference in the stiffness of the relevant modes in graphene.

We now use the calculated values of the phonon lifetime for the optical modes at the Γ point to make comparisons with previously calculated values of the electron-phonon coupling interaction in graphene. From Fig. 4, we obtain that at the Γ point for the in-plane optical modes, $(\tau f)^{-1} \approx 0.8\ \text{fs}^{-1}$ and from Fig. 2, $f(0.5) = 1.5 \times 10^{-3}$ and $f(0.011) = 7.5 \times 10^{-5}$. Then, the value of the phonon lifetime due to ^{13}C impurities (no other lifetime limiting effects included) is $\tau_{\text{ph-imp}} \approx 0.83$ ps for an isotopic atomic density of $\rho = 0.5$ and a value $\tau_{\text{ph-imp}} \approx 16.7$ ps for naturally occurring carbon. Previously calculated results for the electron-phonon coupling at the Γ point of the optical modes[19,20] are on the order $\tau_{\text{e-ph}} \approx 0.6$ ps. Thus it is expected that for high concentrations of isotope impurities, the scattering rates for the isotopic impurity can become as large as that for the electron-phonon interaction. However, for concentrations lower than $\rho = 0.1$, the isotope effect makes only a minor contribution to the phonon lifetime when compared to the electron-phonon interaction for optical phonon modes.

Using the experimental values in Costa *et al.*[5] and assuming the Matthiessen rule holds for the two scattering mechanisms ($\tau^{-1}_{\text{ph}} = \tau^{-1}_{\text{ph-imp}} + \tau^{-1}_{\text{e-ph}}$), we can estimate the contribution of the isotope impurities to the spectral width of the G-band γ_G. We plot in Fig. 5 the experimental values of γ^{exp}_G [full width at half maximum (FWHM)] and taking into account that the spectral width γ is related to the lifetime τ as $\gamma \propto \tau^{-1}$, we fit these values as

$$\gamma_G = \gamma^{\text{exp}}_{\text{e-ph}} + \gamma^{\text{exp}}_{\text{ph-imp}} \frac{f(\rho)}{f(0.5)}, \tag{31}$$

where $f(\rho)$ is defined in Eq. (22), and where we assume that the electron-phonon coupling is the main competing process. The value $\gamma^{\text{exp}}_{\text{ph-imp}}$ obtained from the fitting as defined in Eq. (31) corresponds to the linewidth at a ^{13}C concentration of $\rho = 0.5$. The values obtained from the fitting are $\gamma^{\text{exp}}_{\text{e-ph}} = 11.2 \pm 0.4\ \text{cm}^{-1}$ and $\gamma^{\text{exp}}_{\text{ph-imp}} = 5.2 \pm 0.4\ \text{cm}^{-1}$ and the curve for $\gamma_G(\rho)$ is plotted with dashed lines in Fig. 5. We see that the experimental data are well described by the dashed curve for our model. The in-plane phonon optical modes at the Γ point make the main contribution to the G band in Raman spectroscopy. If we consider our calculated value of the phonon lifetimes at the Γ point of the in-plane optical modes ($\tau_{\text{ph-imp}} \approx 0.83$ ps), and using the uncertainty principle, we obtain $\gamma_{\text{ph-imp}} \approx \hbar/\tau_{\text{ph-imp}} \approx 6.0\ \text{cm}^{-1}$. This result is in good agreement with the experimental result of $5.2\ \text{cm}^{-1}$.

Considering that isotopic defects do not interact directly with electrons, we expect our results to extend to other Raman features. In particular, isotope impurities alone cannot account for the presence of the D band because of the null matrix elements for elastic scattering of the electrons by the isotopic defects. The D band, if present, should originate from other types of defects and the main contribution of ^{13}C atoms would be to shift the D-band frequency due to the mass effect and change the spectral width due to the reduced phonon lifetime.

B. Phonon Localization

To find the phonon localization length, we first compute $A_j = \sum_\mu (\mathbf{e}^\mu_j \cdot \mathbf{e}^\mu_j)^2$ [see Eq. (27)] for random impurities at different impurity concentrations ρ in a supercell. In the previous section, we discussed the case where if the phonon wave function is highly localized, A_j is close to 1, while if it is delocalized, A_j scales as $1/N$. In Fig. 6, we plot the phonon dispersion of graphene as well as the localization length as a function of energy for the different eigenstates and for an impurity density of $\rho = 0.1$ and 0.2. The localization length was normalized by $\lambda_0 = 13$ nm as described in Sec. II C. Here, it is shown that most states will be extended ($\lambda/\lambda_0 \approx 1$) within the size of our supercell, but a few states are localized. These localized states do not occur at random energies but rather occur preferentially at high phonon energies and in regions with flat phonon dispersion (near the M or Γ points). For high frequencies, and in regions with flat phonon dispersions,

backscattering effects become increasingly important and thus localized wave functions are observed. It is in these regions of the spectrum where the localized regime is established when considering phonon transport, as discussed in Savić *et al.*[6] Here we calculate directly the localization length of the wave function using the inverse participation number A_j. Calculated characteristic lengths of a few nanometers for the localization length λ are comparable to those found using a different approach in Savić *et al.*[6] and Yamamoto *et al.*[7] in the high-energy spectrum (in the proximity of 1600 cm^{-1} where the Raman G band is located).

In the case of 1D crystals, it can be shown that all states become localized due to random impurities,[9] and in the case of 2D crystals, a similar behavior is expected as in the 1D case. In the case of 3D crystals, however, a transition from extended to localized states is expected as the energy is moved toward the band edge energies. This shows that localization phenomena are strongly dependent on dimensionality, and therefore careful attention should be paid when comparing results for nanotubes and graphene. Considering that the localized states under consideration have localization lengths on the order of a typical nanotube diameter, the comparison is valid in this case but stops to hold when considering lower frequency phonons with localization lengths on the micrometer scale. In addition, the parameter space when studying localization phenomena in carbon nanotubes is very rich because of the tube diameter and chirality dependence that is not present in graphene.

In this work, we mainly focus on the Γ point of the in-plane optical modes (LO and iTO branches) due to the dominant effect of these modes on the large G-band feature of the Raman spectra. Thus the present size of the supercell is sufficient for our purposes of examining localization effects due to ^{13}C impurities. We also plot in Fig. 6 the calculated values for the out-of-plane phonon modes, where localization effects are also visible in Figs. 6(b) and 6(c) ($\omega \approx 900$ cm^{-1}). Infrared measurements of these modes may provide further information on localization phenomena in this range of frequencies. Even though a softening of the out-of-plane force constants may provide an enhanced effect, it is not clear if this effect will be dominant in an experiment because there will also be an increase of stiffness when considering the interaction of graphene with the substrate (increase of the out-of-plane force constants) or curvature effects if the experiments are done with carbon nanotubes.

In Fig. 7(a), we plot the average localization length λ for optical modes in a phonon frequency interval corresponding to the Γ point of the in-plane optical modes ($\omega \approx 1600$ cm^{-1}) as a function of ^{13}C isotope concentration ρ. From the calculations, a typical localization length is on the order of $\lambda \approx 3$ nm. Examples of the average displacement $|u|$ of the atoms with respect to their equilibrium position as a function of position (projected on the x axis) for localized states are shown in Figs. 7(b) and 7(c) for two samples with $\rho = 0.2$ and 0.4, respectively. Many factors contribute to having an asymmetric curve after averaging over many eigenstates. On the one hand, the effect of increasing the mass of a small number of atoms in the lattice (by adding ^{13}C impurities to a ^{12}C lattice) is not the same as decreasing the mass of a small number of atoms in the lattice (by adding ^{12}C impurities to a ^{13}C lattice). As

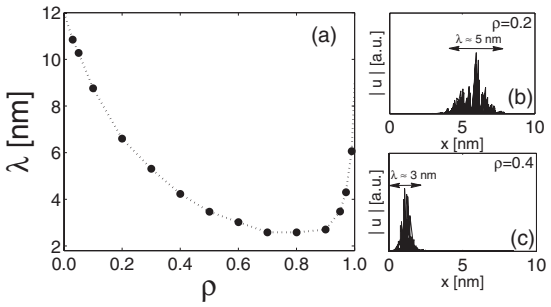

FIG. 7. (a) Localization length λ at the Γ point of the optical phonon modes as a function of ^{13}C atomic density ρ. (b) and (c) Displacement (in arbitrary units) of two different localized eigenstates as a function of position (projected on the x axis) for an in-plane optical mode at the Γ point and corresponding to ^{13}C concentrations of (b) $\rho = 0.2$ and (c) $\rho = 0.4$.

discussed before, the localization length is calculated from the inverse participation number A_j since $\lambda_j \propto A_j^{-1/2}$, and A_j is calculated using the amplitudes of the atoms in the eigenstate j. When we decrease the mass of a small number of atoms, the amplitude of these atoms with decreased mass within some (optical) eigenstate will be larger than the corresponding amplitude of the eigenstate in the pristine samples, and the opposite happens when increasing the mass of a small number of atoms. Therefore even though in both cases the participation number will be larger than the one corresponding to the pristine sample eigenstates, the effect of isotope doping will be more abrupt in the first (decreasing mass) case. In addition, as the frequency of an oscillator scales with mass m as $\propto m^{-1/2}$, when we change the ^{13}C density of the sample, there are considerable changes in the density of states and therefore, when averaging over a frequency window, the comparison of localization lengths λ at different densities ρ is not straightforward. The physics behind the localization of the eigenstates is related to the formation of islands that vibrate at a different frequency from the rest of the lattice. At a 3-nm-length scale, for example, around 100 atoms are vibrating in the localized mode and this regime corresponds to the case of weak localization.[21]

C. Further interactions

In this work, we only considered ^{13}C impurity scattering, and disregarded all other kinds of scattering events. The objective of this approach was to obtain the characteristic lifetimes associated with the ^{13}C impurity. In this way, it is possible to compare the effect of this scattering process with all other competing processes to determine the relative importance of each. We compared our results for the ^{13}C isotopic impurity scattering process with previously calculated values of the electron-phonon interaction which is an important process when considering optical phonons modes and their effect on the Raman spectra. Another potentially important term is the inclusion of anharmonic effects, which are associated with the thermal expansion of the lattice and such effects are observable through temperature-dependent Raman spectroscopy[22] studies, usually included in molecular dynamics simulations and are also important in phonon transport,[23] which will be

a future work. Because of the temperature dependence of the anharmonic terms, such effects can, in principle, be tuned and accounted for in an experiment. In addition, inclusion of other types of defects like vacancies, grain boundaries, dislocations, etc., is also necessary, and understanding the relative importance of each of these scattering processes on the phonon modes as a function of temperature and other parameters remains to be investigated both theoretically and experimentally. In principle, static point defects such as substitutional atoms can be studied using a similar approach as the one used in this paper, while extended defects such as grain boundaries or dislocations require a different treatment.

IV. CONCLUSIONS

In the present work, we studied the effects of ^{13}C isotope doping on the optical phonon modes of graphene. Here, we calculated the values of the phonon lifetimes due to isotope impurity scattering for all values of ^{13}C densities and for all wave vectors within second-order perturbation theory. Phonon lifetimes of optical phonon modes are considerably smaller (0.8 ps) than the corresponding lifetimes of the acoustic modes (which scale as a power law of the frequencies). We found that for natural concentrations of ^{13}C, the contribution of isotopic scattering of optical modes is negligible when compared to the electron-phonon interaction. Nevertheless, for atomic concentrations as high as $\rho = 0.5$, both contributions become comparable. Our results were compared with recent experimental results of ^{13}C Raman spectroscopy of nanotubes and good agreement was found for both the density dependence of the lifetime as well as in the calculated spectral width of the G band. We predicted that the reduction of phonon lifetimes by changing ^{13}C isotopes to ^{14}C would be approximately fourfold.

The localization of optical phonons due to isotope impurities in graphene is calculated by the supercell method. Due to phonon scattering by ^{13}C isotopes, some graphene wave functions become localized in real space. Localized states appear predominantly in the high-energy optical phonon modes and in regions of flat phonon dispersion, where backscattering effects become increasingly important. A typical localization length is on the order of 3 nm for optical phonon modes at high concentrations of ^{13}C (in the range of number densities $\rho =$ 0.2–0.8). Even though we focused attention mostly on in-plane optical modes, out-of-plane phonon modes may also provide a way to measure phonon localization effects and can be studied experimentally by infrared measurements. Even though these modes may also show pronounced localization effects due to reduced out-of-plane force constants, the coupling of graphene with the substrate (or curvature effects when considering nanotubes) may introduce more complicated effects.

There are still many issues for further study. Even though there has been a considerable amount of work done related to electron-phonon coupling, inclusion of anharmonic effects and phonon-defect interactions are also important for understanding phonon-related processes in Raman spectroscopy[24] and in phonon transport more generally. In particular, substitutional defects, vacancies, grain boundaries, and edges may make an important contribution to the overall phonon scattering processes. Calculating the relative importance of these interactions in the full parameter space, including the temperature dependence, is relevant not only for basic science, but also for technological applications.

ACKNOWLEDGMENTS

We thank Professors M. A. Pimenta, D. A. Broido, and N. Mingo for useful discussions. The MIT authors acknowledge NSF Grant No. DMR-10-1004147. R.S. acknowledges MEXT grant No. 20241023. S.D.C. acknowledges the fellowship from the Brazilian Agency CAPES for the postdoctoral research at UFMG.

[1] Y. Miyauchi and S. Maruyama, Phys. Rev. B **74**, 035415 (2006).
[2] S. Fan, L. Liu, and M. Liu, Nanotechnology **14**, 1118 (2003).
[3] X. Li, W. Cai, L. Colombo, and R. S. Ruoff, Nano Lett. **9**, 4268 (2009).
[4] M. Kalbac, H. Farhat, J. Kong, P. Janda, L. Kavan, and M. S. Dresselhaus, Nano Lett. **11**, 1957 (2011).
[5] S. D. Costa, C. Fantini, A. Righi, A. Bachmatiuk, M. H. Rümmeli, R. Saito, and M. A. Pimenta, Carbon **49**, 4719 (2011).
[6] I. Savić, N. Mingo, and D. A. Stewart, Phys. Rev. Lett. **101**, 165502 (2008).
[7] T. Yamamoto, K. Sasaoka, and S. Watanabe, Phys. Rev. Lett. **106**, 215503 (2011).
[8] P. W. Anderson, Phys. Rev. **109**, 1492 (1958).
[9] B. Kramer and A. MacKinnon, Rep. Prog. Phys. **56**, 1469 (1993).
[10] D. S. Wiersma, P. Bartolini, A. Lagendijk, and R. Righini, Nature (London) **390**, 671 (1997).
[11] P. E. Lindelof, J. Nørregaard, and J. Hanberg, Phys. Scr. **1986**(T14), 17 (1986).
[12] A. C. Ferrari, Solid State Commun. **143**, 47 (2007).
[13] A. H. Castro Neto and F. Guinea, Phys. Rev. B **75**, 045404 (2007).
[14] R. A. Jishi, L. Venkataraman, M. S. Dresselhaus, and G. Dresselhaus, Chem. Phys. Lett. **209**, 77 (1993).
[15] E. B. Barros, K. Sato, Ge. G. Samsonidze, A. G. Souza Filho, M. S. Dresselhaus, and R. Saito, Phys. Rev. B **83**, 245435 (2011).
[16] F. Wegner, Z. Phys. B **36**, 209 (1980).
[17] P. G. Klemens, Proc. Phys. Soc., London, Sec. A **68**, 1113 (1955).
[18] L. Lindsay, D. A. Broido, and N. Mingo, Phys. Rev. B **83**, 235428 (2011).
[19] J. Jiang, R. Saito, A. Grüneis, G. Dresselhaus, and M. S. Dresselhaus, Chem. Phys. Lett. **392**, 383 (2004).
[20] J. Jiang, R. Saito, Ge. G. Samsonidze, S. G. Chou, A. Jorio, G. Dresselhaus, and M. S. Dresselhaus, Phys. Rev. B **72**, 235408 (2005).
[21] J. M. Ziman, *Models of Disorder: the Theoretical Physics of Homogeneously Disordered Systems* (Cambridge University Press, Cambridge, 1979).
[22] I. Calizo, A. A. Balandin, W. Bao, F. Miao, and C. N. Lau, Nano Lett. **7**, 2645 (2007).
[23] L. Lindsay, D. A. Broido, and N. Mingo, Phys. Rev. B **82**, 115427 (2010).
[24] P. Venezuela, M. Lazzeri, and F. Mauri, Phys. Rev. B **84**, 035433 (2011).